Journal of Applied Physics

RESEARCH ARTICLE | AUGUST 21 2023

Multifunctional fluorescent nanocomposite of PVDF-TrFE and europium barium titanate

Christine K. McGinn ; Nasim Farahmand ; Stephen O'Brien ; Ioannis Kymissis

J. Appl. Phys. 134, 074103 (2023)
https://doi.org/10.1063/5.0150084

AIP Publishing

Journal of Applied Physics ARTICLE pubs.aip.org/aip/jap

Multifunctional fluorescent nanocomposite of PVDF-TrFE and europium barium titanate

Cite as: J. Appl. Phys. **134**, 074103 (2023); doi: 10.1063/5.0150084
Submitted: 11 March 2023 · Accepted: 29 July 2023 ·
Published Online: 21 August 2023

Christine K. McGinn,[1,a)] Nasim Farahmand,[2] Stephen O'Brien,[2] and Ioannis Kymissis[1]

AFFILIATIONS

[1]Department of Electrical Engineering, Columbia University, New York, New York 10027, USA
[2]Department of Chemistry and Biochemistry, The City College of New York, New York, New York 10031, USA

[a)]**Author to whom correspondence should be addressed:** cm3592@columbia.edu

ABSTRACT

Polyvinylidene difluoride trifluoroethylene (PVDF-TrFE) has received widespread application in flexible electronics and biomedical devices but is limited in its sensing modalities to piezoelectricity and pyroelectricity. The addition of optically or magnetically active nanoparticles could provide additional sensing modalities in the same element, which could drive miniaturization of such sensors. Europium barium titanate (EBTO) is one such optically active nanoparticle that could add functionality to such a nanocomposite. In this work, multifunctional nanocomposites of PVDF-TrFE and EBTO are successfully synthesized and characterized for their material and electronic properties. The nanocomposite in this work is the first known multifunctional nanocomposite with PVDF-TrFE and a fluorescent nanoparticle.

I. INTRODUCTION

Increased interest in flexible electronics, a desire to find lead-free alternatives for energy harvesting, and increased functionality and commercial availability of nanoparticles have driven new interest in piezoelectric nanocomposites.[1–4] Flexible electronics for biomedical and healthcare applications, in particular, have seen significant advances in the last decade.[5–8] Both polyvinylidene difluoride (PVDF) and its copolymer polyvinylidene difluoride trifluoroethylene (PVDF-TrFE) are widely utilized in these applications as they have a unique combination of characteristics of being biocompatible, transparent, and flexible in addition to having significant piezoelectric and pyroelectric coefficients.[9] Their piezoelectric and pyroelectric character is key for the operation of wearable heart rate and blood pressure sensors for e-skin applications.[10–13] The high dielectric constant of PVDF-TrFE is also desirable for flexible electronic devices, especially mechanical sensors.[14,15] PVDF-TrFE additionally occupies a unique place in the energy harvesting as it is solution processable and its piezoelectric coefficient (d_{33}) is higher than almost any other lead-free piezoelectric.[16]

The drive to study nanocomposites with PVDF-TrFE was initially driven by the desire to create a material for energy harvesting that combines the processing advantages of PVDF-TrFE and the higher piezoelectric coefficient of ceramic piezoelectric materials like lead zirconate titanate and barium titanate.[17–21] Particular interest has been paid to creating a lead-free composite that can begin to approach the performance of lead zirconate titanate without the concern for toxicity.[4,22] There have been several successful demonstrations of showing modest improvement of the piezoelectric and ferroelectric character in nanocomposite materials based on PVDF-TrFE for energy harvesting.[23–25] In addition to improved piezoelectric coefficients, barium titanate has a higher pyroelectric coefficient than PVDF-TrFE that is desirable for tactile sensor applications.[26]

While the bulk of past work on PVDF-TrFE nanocomposites focuses on improving piezoelectric and pyroelectric character, some researchers have begun to consider creating multifunctional nanocomposite materials to support miniaturization by combining multiple functionalities in one component.[27,28] Such miniaturization is ideal for wearable and Internet of Things applications where multiple types of sensors are integrated into one device or system. As PVDF-TrFE is biocompatible, it is ideal for creating multifunctional sensors for healthcare applications. Two significant works have explored the idea of a multifunctional nanocomposite, but both investigated sensing of pressure and temperature simultaneously using pyroelectric and ferroelectric nanoparticles rather than incorporating a new functionality to PVDF-TrFE.[28–30] Gupta *et al.* synthesized a barium titanate and PVDF-TrFE nanocomposite to perform real-time touch and temperature monitoring for e-skin

applications.[28] The addition of barium titanate nanoparticles provides a small increase to the capacitance of the PVDF-TrFE, which gives modest improvements to the piezoelectric and pyroelectric response to track temperature and pressure. In Ref. 30, lead titanate nanoparticles are successfully poled opposite to the poling direction of the PVDF-TrFE host. The pyroelectric and piezoelectric response is then differentiated by comparing devices with aligned and misaligned nanoparticle polarization.[30] In both works, the nanoparticle helps us to isolate two different existing responses in PVDF-TrFE, the pyroelectric and piezoelectric response, rather than imparting a new functionality. A few works have studied adding a new functionality to PVDF-TrFE by using optically active nanoparticles to PVDF-TrFE, but these works only focused on improving the optical sensing capabilities of the nanocomposite rather than using the host and nanoparticle materials to perform multiple types of sensing.[31] Nanoparticles with a wide range of optical and magnetic properties have been prepared as the fillers for PVDF-TrFE nanocomposites, with the goal of adding new and interesting properties.[32–34] There is ample room to further pursue the design of multifunctional nanocomposites with PVDF-TrFE that can advance sensor functionalities and miniaturization by performing multiple modalities of sensing simultaneously.

Europium barium titanate (EBTO) nanoparticles are one such optically active material, which could be leveraged for a multifunctional nanocomposite with PVDF-TrFE. EBTO demonstrates fluorescence with absorption at 240 nm and emission at 620 nm.[35] Eu^{3+} is a spectrally narrow core state electronic transition, which is well-isolated from both the ceramic and the polymer. With an absorption in the ultraviolet range and an emission in the visible range, a PVDF-TrFE/EBTO nanocomposite could have dual simultaneous functions as a solar-blind UV sensor and pressure or temperature sensor, which would be useful for healthcare and Internet of Ihings applications. However, several materials challenges will need to be overcome to achieve such a nanocomposite. EBTO nanoparticles are large size nanoparticles with a diameter of 100 nm, which could substantially interrupt the ferroelectric and piezoelectric properties of the PVDF-TrFE. Previous work has shown that this interruption can be significant.[36] There is also an opportunity for PVDF-TrFE to quench the fluorescence of the EBTO nanoparticles. Applying any electric field to the PVDF-TrFE/EBTO nanocomposite will compound the high electric field due to the remnant polarization of PVDF-TrFE and, thus, expose the EBTO nanoparticle to exceptionally high fields. These high electric fields may alter the Eu^{3+} core state and affect the optical fluorescence. No such effect has been seen in the literature so any effect would be of general scientific interest. If the state is unaffected by the high fields and this core state remains unaffected under such high fields, then optical and electronic sensing can be done independently by the film, yielding a truly multifunctional nanocomposite.

The nanocomposite in this work is the first multifunctional nanocomposite with PVDF-TrFE and a fluorescent nanoparticle. Several concentrations of PVDF-TrFE/EBTO nanocomposites were

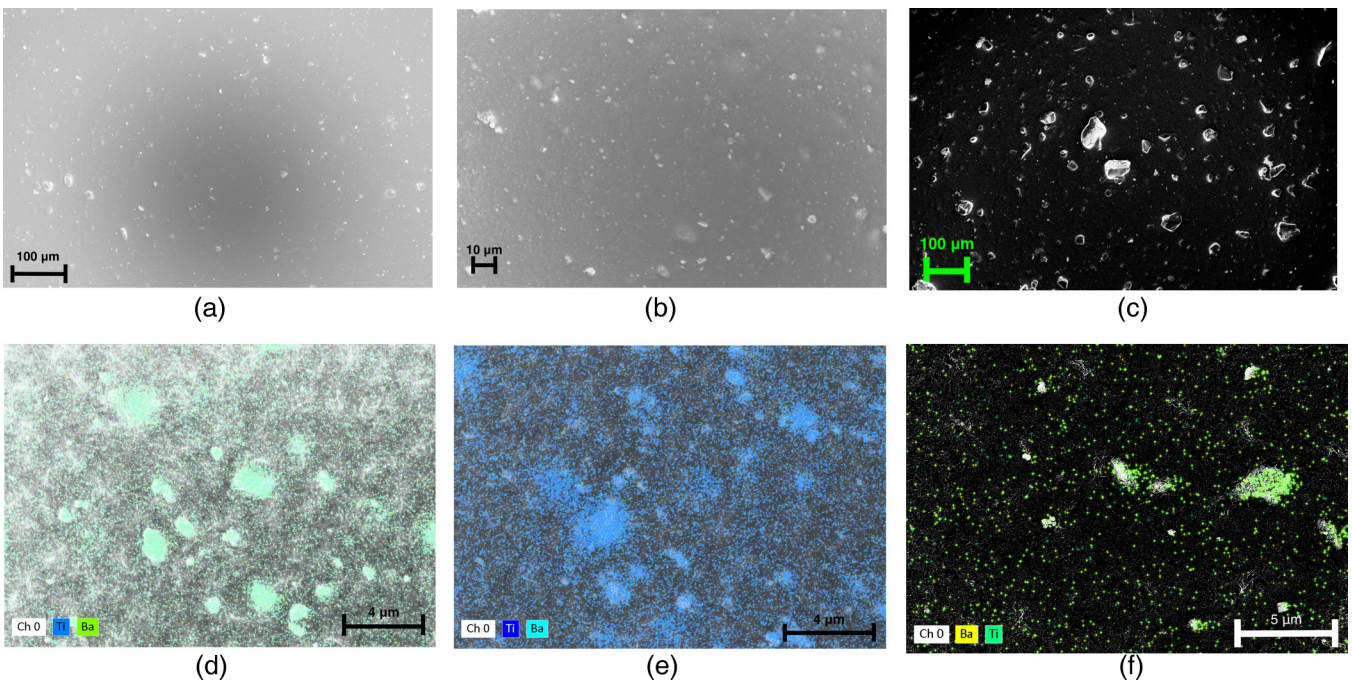

FIG. 1. (a) SEM image of 5 wt. % PVDF-TrFE/EBTO nanocomposite. (b) SEM image of 10 wt. % PVDF-TrFE/EBTO nanocomposite. (c) SEM image of 20 wt. % PVDF-TrFE/EBTO nanocomposite. (d) EDS image showing the location of barium and titanium for 5 wt. % sample, signifying the possible presence of a nanoparticle. (e) EDS image for 10 wt. % sample. (f) EDS image for 20 wt. % sample.

investigated in this work both to investigate their material properties and determine the best nanocomposite mixture for creating a multifunctional nanocomposite. The resulting materials were then characterized for their dielectric, ferroelectric, piezoelectric, and electro-optical properties.

II. NANOCOMPOSITE PREPARATION

The nanocomposite mixture was prepared using a simple mixing procedure adapted from previous studies on PVDF-TrFE nanocomposites. All nanocomposites contained 20 wt. % PVDF-TrFE. To encourage good dispersion of the EBTO nanoparticles in the resulting nanocomposite film, the EBTO nanoparticles (approximately 100 nm in diameter) were first mixed into the chosen solvent, dimethyl formamide (DMF), before the addition of PVDF-TrFE. After adding the nanoparticles to the solvent, it was sonicated for 30 min to encourage even dispersion. Typical mixtures contained 200–500 mg of EBTO nanoparticles and 1–1.25 g of PVDF-TrFE to create a 5, 10, and 20 wt. % solution of EBTO to PVDF-TrFE and 20 wt. % solution of PVDF-TrFE to DMF. Once mixing was completed, the mixture was placed a hot plate at 30 °C and stirred with a magnetic stir bar for 15 min to encourage mixing. The heat was then turned off and the solution was allowed to mix overnight. Films were cast onto the substrates via spin-coating. 20 wt. % solutions were spin-coated at 1500 rpm to create films of 5–7 μm thick. 5 and 10 wt. % solutions were spin-coated at 3000 rpm to create films of 2–5 μm thick. The spin-coating speed was increased for lower concentration solutions to lower the needed poling voltage. To evaporate the solvent, the sample was heated in a hot place at 90 °C for 10 min before being moved to an oven at 135 °C for an hour to encourage crystallization into the β phase. Samples prepared for electronic measurements were prepared with Cr/Al (5/100 nm) contacts on top and bottom of the nanocomposite film. For the optoelectronic measurement, only 5 nm of Al was used as the top electrode to allow light to pass through the top electrode. These films were poled using a stepwise method with a maximum electric field of 100 V/μm.[37]

Energy dispersive x-ray spectroscopy (EDS) was then performed on the sample to verify the degree of nanoparticle dispersion in the film. The location of barium, titanium, and oxygen was used as an approximate measure of the nanoparticle positions. The first sample measured was the 20 wt. % solution, and an SEM image of the surface at low magnification is shown in Fig. 1(c). From this image, it is evident that the dispersion is poor as the nanoparticles have created clusters as large as 100 μm. A focused image shown in Fig. 1(f) confirms the poor dispersion.

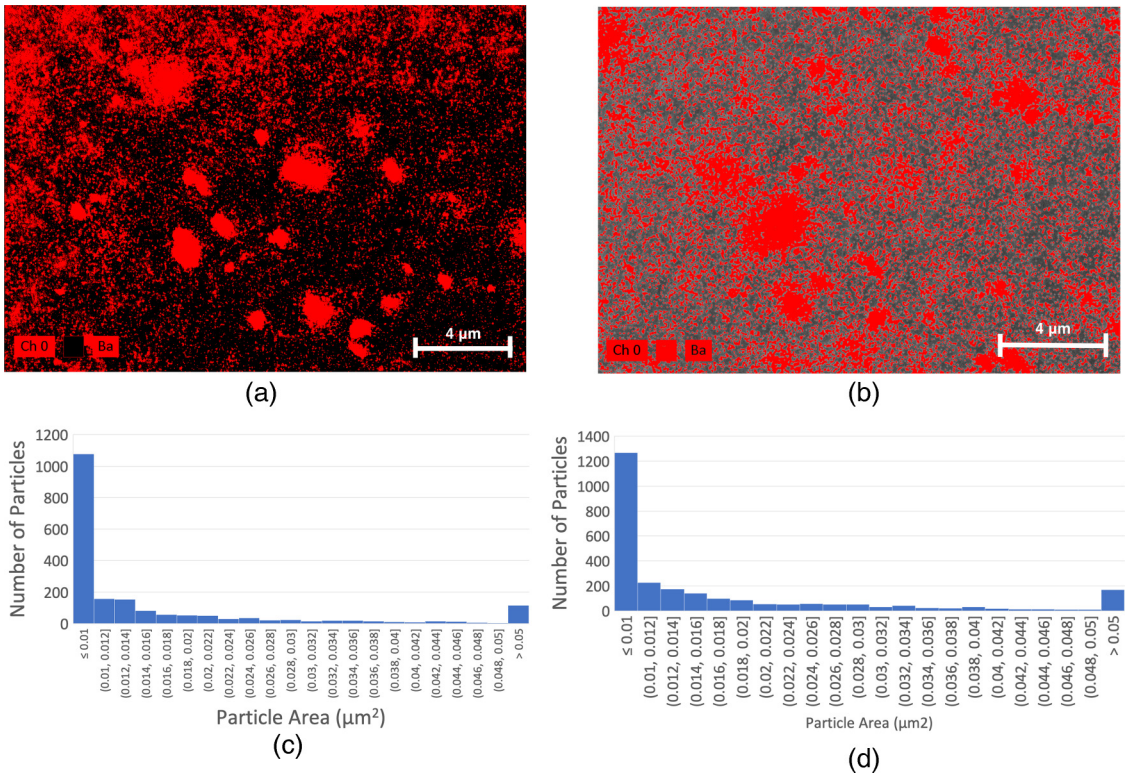

FIG. 2. Analysis of SEM EDS images: (a) PVDF-TrFE/EBTO 5 wt. % image with particles and particle clusters identified, (c) histogram of particle cluster sizes by area for PVDF-TrFE/EBTO 5 wt. % film, and (d) histogram of particle cluster sizes by area for PVDF-TrFE/EBTO 10 wt. % film.

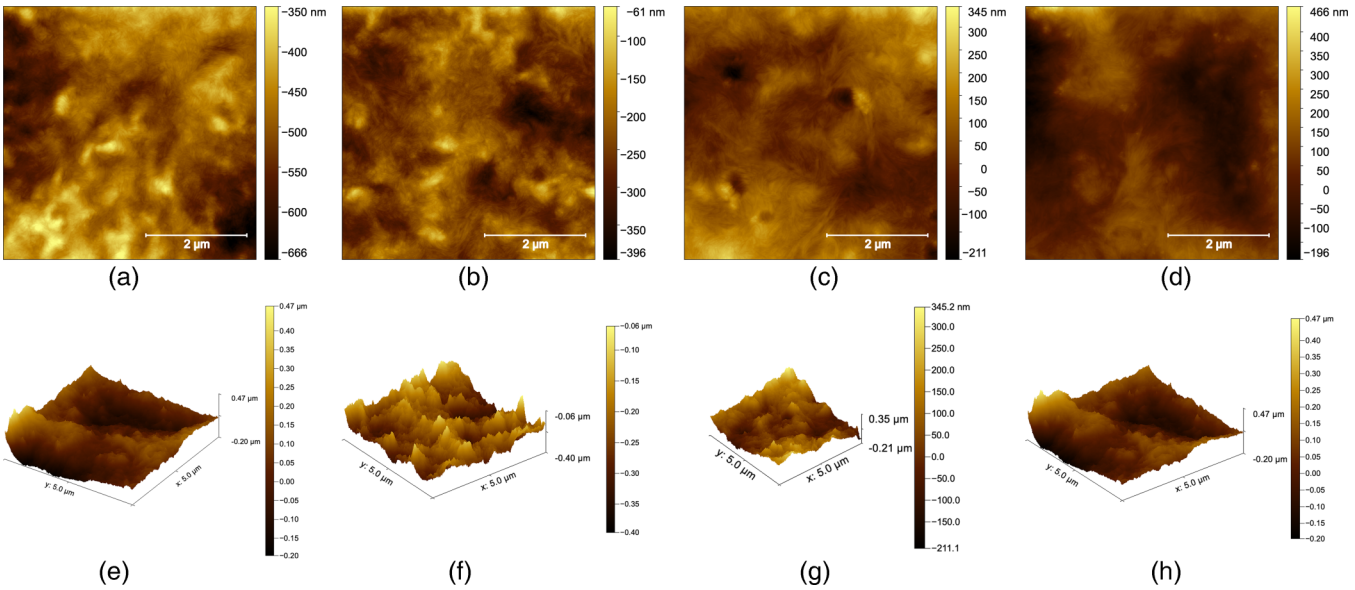

FIG. 3. Atomic force microscopy images of EBTO nanocomposites: (a) PVDF-TrFE, (b) PVDF-TrFE/EBTO 5 wt. %, (c) PVDF-TrFE/EBTO 10 wt. %, and (d) PVDF-TrFE/EBTO 20 wt. % 3D. Atomic force microscopy images of EBTO nanocomposites: (a) PVDF-TrFE, (b) PVDF-TrFE/EBTO 5 wt. %, (c) PVDF-TrFE/EBTO 10 wt. %, and (d) PVDF-TrFE/EBTO 20 wt. %.

After these observations, several changes were made to the mixing procedure to create more homogeneous films for lower concentrations of EBTO. Vortex mixing was done throughout the addition of PVDF-TrFE, and an additional sonication step of 15–30 min was performed after all components of the solution were added. After mixing overnight, a final sonication step of 10–15 min was added before spin-coating.

Characterization of these films by SEM imaging and EDS showed a marked improvement in the dispersion due to the combination of lower nanoparticle concentration and changes to the mixing procedure. The SEM images of the 5 and 10 wt. % samples can be seen in Figs. 1(a) and 1(b), respectively. In these images, it can be seen that the improvements in the film processing decreased the size of the largest nanoparticle clusters by ten times. EDS images in Figs. 1(d) and 1(e) show a similar level of dispersion in both 5 and 10 wt. % EBTO samples and a significant improvement over the 20% sample given the increased density of barium and titanium signatures throughout the image. To further understand the difference in dispersion between the 5 and 10 wt. % EBTO concentrations, ImageJ was used to perform image processing to identify the cluster areas based on the EDS images. The processed images and histograms are shown in Fig. 2. From the histograms, it can be seen that the 5 wt. % sample skews slightly more toward smaller clusters, which may indicate slightly better dispersion. Additionally, there are almost the same number of the smallest clusters despite the 5 wt. % sample having half as many nanoparticles by weight.

Atomic force microscopy (AFM) was used to further assess the dispersion by analyzing the surface roughness of each film and providing a macroscopic assessment of the dispersion. Flattened AFM scans of the surface of each nanocomposite film are shown with associated 3D images in Fig. 3. The calculated surface roughness of each sample is shown in Table I. These data correspond to the assessment of the dispersion from the EDS analysis as the surface roughness of the 20 wt. % sample is almost two times higher than that of the 5 and 10 wt. % samples, which was lower than the surface roughness of the pure PVDF-TrFE films. From these data, it was determined that the EBTO nanoparticles were sufficiently dispersed in the film as the surface roughness of the 5 and 10 wt. % samples were lower than that of pure PVDF-TrFE.

III. X-RAY DIFFRACTION

X-ray diffraction was used to ensure the crystallinity of the PVDF-TrFE remained in the β phase after the addition of the EBTO samples. As the β phase is the most electroactive phase of PVDF-TrFE, it is critical for a nanocomposite to maintain this crystallinity to provide the piezoelectric effect needed for multifunctionality. The β crystalline phase is a mixture of the mixture of the (110) and (200) crystalline directions and signified by a single peak at approximately 20°.[38] The resulting XRD data in

TABLE I. Comparison of RMS roughness for PVDF-TrFE/EBTO nanocomposites.

Concentration of EBTO (wt. %)	RMS roughness
0	37.0
5	36.7
10	36.7
20	63.1

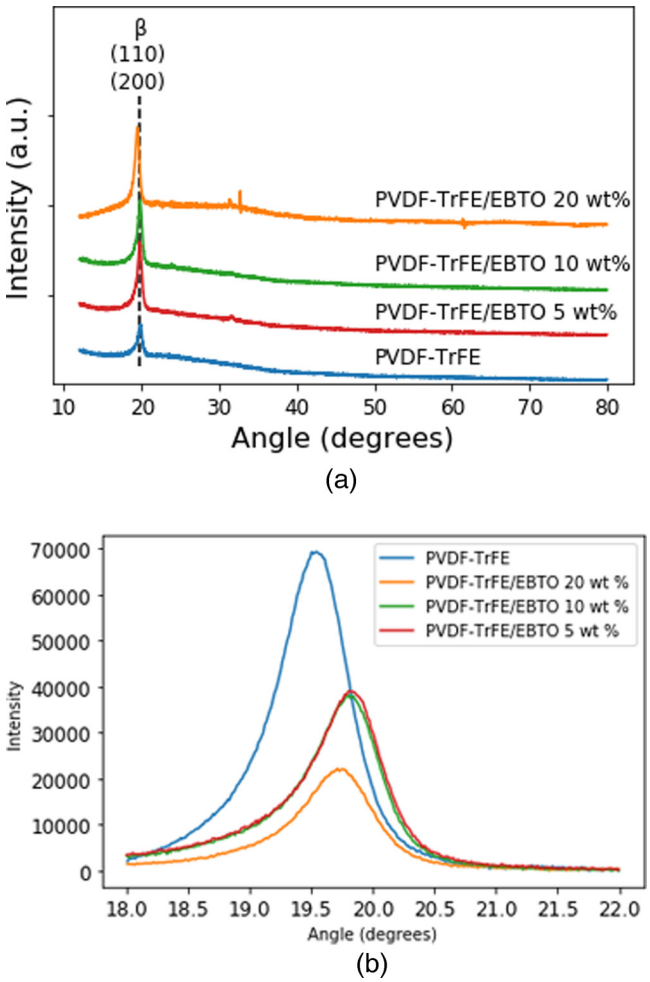

FIG. 4. (a) Broad range x-ray diffraction scan of PVDF-TrFE/EBTO samples with comparison to pure PVDF-TrFE sample. (b) Shortened x-ray diffraction scan showing β phase peaks of all PVDF-TrFE/EBTO samples.

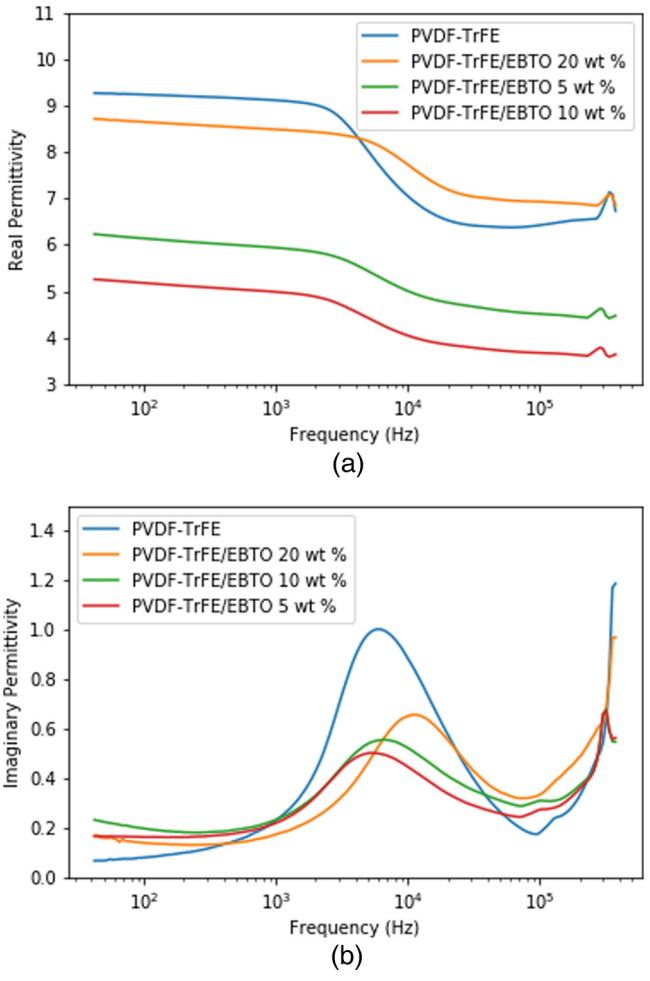

FIG. 5. Ferroelectric hysteresis of PVDF-TrFE/EBTO nanocomposites.

comparison to pure PVDF-TrFE is shown in Fig. 4(a). A comparison of the β phase peak at 20° for all samples is shown in Fig. 4(b). All samples maintained the β phase signature at 20°. The slight shift in the location of the signature peak represents a slight increase in the (200) component of the crystallinity. The decrease in peak intensity is likely due to the volumetric replacement of EBTO in the film as it decreases with increasing concentration.

IV. ELECTRICAL CHARACTERIZATION

After observing sufficient dispersion of the nanoparticles and preservation of the PVDF-TrFE β phase, the samples were evaluated for their ferroelectric, dielectric, and piezoelectric properties to identify their performance for a multifunctional nanocomposite.

A. Ferroelectric measurement

The ferroelectric behavior of the films was observed first as ferroelectricity only results from proper sample preparation and is foundational to the pyroelectric and piezoelectric characteristics of PVDF-TrFE. Ferroelectric hysteresis curves are also used to identify the coercive field needed for poling to maximize the piezoelectric coefficient of the films. A radiant ferroelectric materials tester was used to observe the ferroelectric hysteresis loops of each nanocomposite and a pure PVDF-TrFE film, and the results are shown in Fig. 5.

For all PVDF-TrFE/EBTO nanocomposites, the maximum polarization is less than that of the pure polymer but decreases with decreasing concentration. A decrease from the pure polymer for the nanocomposite is generally expected as the nanoparticles replace some volume of the PVDF-TrFE and disrupt the crystallinity locally. Although EBTO itself is ferroelectric, it has been shown that the ferroelectric contribution of nanoparticles is not enough to

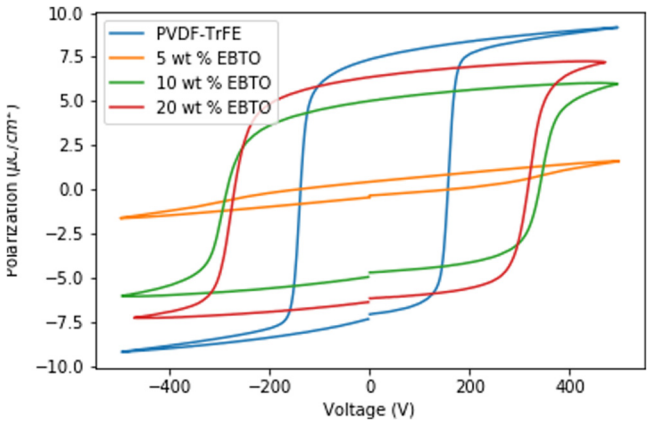

FIG. 6. (a) Real permittivity of PVDF-TrFE/EBTO nanocomposites. (b) Imaginary permittivity of PVDF-TrFE/EBTO nanocomposites.

compensate for the volumetric replacement in PVDF-TrFE nanocomposites.[36]

There is a marked difference between the 5 and 10 wt. % films despite the materials characterization performed via EDS and AFM indicating that the 5 and 10 wt. % films had similar degrees of nanoparticle distribution and β phase crystallinity.

B. Dielectric constant

Next, the dielectric constant of the nanocomposites was measured using an impedance analyzer to determine the film's dielectric strength and electronic stability. The resulting measurements are shown in Fig. 6. The real permittivity of the 20 wt. % film is similar to that of PVDF-TrFE itself. Its bulk capacitance may be similar to that of the pure polymer because the clustering of nanoparticles in the film leaves large portions of the polymer structure undisturbed. The real permittivity of both the 5 and 10 wt. % films is approximately 30%–50% lower than that of the pure polymer. This trend is consistent with previous observations of the material characteristics of each nanocomposite concentration. All of the nanocomposite films show less loss than the pure polymer but are mostly indistinct from each other.

C. Piezoelectric coefficient

For a truly multifunctional nanocomposite, it is critical that the nanocomposite retain the piezoelectricity contributed by PVDF-TrFE. To test the piezoelectric coefficient, the films were stimulated with 9 V_{pp} sinusoidal input from 200 Hz to 100 kHz and the piezoelectric response was observed with a laser vibrometer. A wide range of frequencies were measured to avoid any potential resonance frequencies.[39] The d_{33} value at each frequency was then obtained by dividing the maximum displacement observed by the laser vibrometer by the input voltage. The overall d_{33} value was determined by averaging the d_{33} values below 10 kHz. This point was chosen as it is when the dielectric constant of the film degrades by over 10% of its value at approximately 100 Hz. The results are shown in Table II.

TABLE II. Piezoelectric coefficients for PVDF-TrFE/EBTO nanocomposites.

Sample	d_{33} (pC/N)	Error
Reference	0.2092	0.3651
PVDF-TrFE	39.2303	8.1191
PVDF-TrFE/EBTO 5 wt. %	4.1713	0.3204
PVDF-TrFE/EBTO 10 wt. %	27.4524	5.2530
PVDF-TrFE/EBTO 20 wt. %	16.8557	3.8315

Each nanocomposite retains some piezoelectric character, but 10 wt. % EBTO appears to be the optimal concentration to provide reasonable dispersion throughout the film while still maintaining most of the piezoelectric response of PVDF-TrFE.

V. ELECTRO-OPTICAL MEASUREMENT

A major question of this work is whether the fluorescence of EBTO nanoparticles can be affected by the high fields possible inside of PVDF-TrFE, which would diminish the effectiveness of the multifunctional nanocomposite. A schematic of the optical experiment used to define the electro-optical response is shown in Fig. 7(b). A 275 nm LED source was used to excite the EBTO nanoparticles in the nanocomposite, and the resulting 610–620 nm fluorescence was captured with a multimode fiber. The light captured by the multimode fiber was then passed through 400 nm longpass filter before being observed with a photodetector to ensure that no incident light would be observed. A lock-in amplifier was used to modulate the LED source and observe the resulting fluorescence through the photodetector. The lock-in amplifier can sense femptoamp changes in the output signal, so even small changes in the fluorescence due to an applied electric field should be observed. A source measurement unit was used to apply a voltage across the nanocomposite film to create a large field in the film. The real-time fluorescence strength as observed by the photodetector and lock-in amplifier to input voltages of 5, 20, and 50 V is shown in Fig. 7(c). The 10 wt. % EBTO sample was used for this experiment as it had the highest combined piezoelectric coefficient and remnant polarization and, thus, would have the greatest effect on the EBTO nanoparticle fluorescence if any could be observed.

With an applied voltage above 5 V, there is an observable change in the fluorescence from the EBTO nanoparticles in the nanocomposite film. This change is only approximately 10% of the overall fluorescence signal with no voltage applied. While a linear quenching effect would be expected for increasing fields, the quenching seems to show more of an ON/OFF behavior.

VI. DISCUSSION

For the concentrations tested, only 5 and 10 wt. % EBTO demonstrated sufficient dispersion as shown by both EDS analysis and AFM surface roughness measurements. All samples maintained the β phase signature of a lone peak at approximately 20° in XRD measurements. The shift in peak location indicates that the addition of the nanoparticle might foster more (200) than (110) content in the film.[38] Changes in the intensity of the peak are likely due to the volumetric replacement of EBTO in the film. The films then had

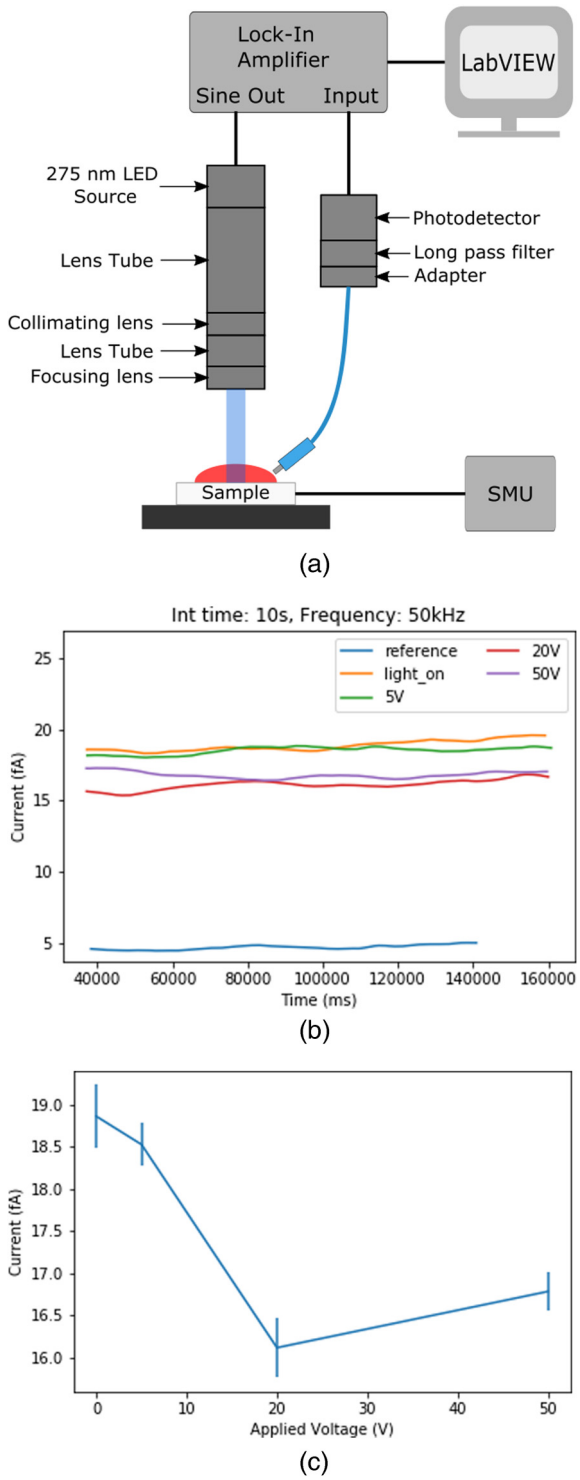

FIG. 7. (a) Setup for electro-optical measurement. (b) Real-time fluorescence strength for several applied voltages. (c) Response against voltage applied.

sufficient dispersion and crystallinity for a multifunctional nanocomposite.

The remnant polarization for the films decreased with decreasing concentration. No real trend was observed among the three nanocomposites for the dielectric constant. The 20 wt. % solution yielded a response closest to that of PVDF-TrFE. A possible explanation is that the nanoparticles were sufficiently clumped together in the film that it caused very little disruption to the polymer's response. Using this logic, the difference in response for both ferroelectric and dielectric measurements between the 5 and 10 wt. % may indicate that the dispersion is not as similar as suggested by the AFM and EDS results. Image processing on the SEM EDS images shows that the 5 wt. % sample has slightly better dispersion to support this hypothesis. As both AFM and EDS are limited to a two-dimensional analysis, more work should be done to investigate the local dispersion throughout the film to understand this trend.

Each film did have a measurable d_{33} coefficient signaling piezoelectric behavior. The piezoelectric response for the 5 wt. % sample was the lowest, but this result does correlate with the low remnant polarization observed in the ferroelectric hysteresis measurement as the piezoelectric constant arises from aligning the available dipoles in the film. Further materials characterization would need to be done to understand why the 5 wt. % solution yields such different electronic behavior from the 10 wt. % solution despite minute material characteristics. The 10 wt. % sample has the closest d_{33} to the pure polymer of the three concentrations tested. The 10 wt. % sample then best retained the electronic behavior of PVDF-TrFE while also having sufficient nanoparticle dispersion. This sample then was used in the electro-optical measurement to test its viability as a multifunctional composite as it would yield the highest electric fields and, thus, provide the biggest possible disruption to the fluorescence of the EBTO nanoparticle.

The observed change in fluorescence of the EBTO nanoparticle in the composite film is very small at less than a 10% change in signal but is observable for an applied voltage above 5 V. The change demonstrated with 20 and 50 V applied would still enable multifunctional use of the nanocomposite as few applications would require such high voltage, but is interesting on its own as modulation of the Eu^{3+} fluorescence by an electric field has not been previously reported. This change is likely due to the compounding effects of the electric field due to the remnant polarization in the film and the large fields that can be applied to PVDF-TrFE. The damping effect observed does show an ON/OFF effect rather than the linear effect that would be expected. The fluorescence quenching should be studied further to understand the nonlinear behavior observed and exactly quantify the effect.

VII. CONCLUSION

Several concentrations of PVDF-TrFE/EBTO nanocomposites were studied to obtain a multifunctional nanocomposite. 10 wt. % EBTO solution was best able to retain the desired electronic characteristics of PVDF-TrFE with sufficient dispersion of nanoparticles throughout the film. The ferroelectric, dielectric, and piezoelectric character was diminished for all nanocomposites in comparison to

pure PVDF-TrFE despite preservation of the β phase crystallinity. Some quenching of the fluorescence of EBTO was observed when high electric fields were applied, but the effect is small and nonlinear. As both the piezoelectric response of the polymer and the fluorescence of the EBTO are largely retained in the nanocomposite, this nanocomposite is one of the first truly multifunctional nanocomposites demonstrated in the literature, and the first known multifunctional nanocomposite with PVDF-TrFE and a fluorescent nanoparticle. The characterization shown in this work demonstrates that the fabricated multifunctional nanocomposite can be used for both optical and piezoelectric or pyroelectric sensing simultaneously, which can be leveraged for miniaturization of sensors for Internet of Things and wearable applications.

ACKNOWLEDGMENTS

The authors first wish to thank Professor Elizabeth Olson for expert guidance on the laser vibrometer measurements. The authors acknowledge the use of facilities and instrumentation supported by NSF through the Columbia University, Columbia Nano Initiative, and the Materials Research Science and Engineering Center DMR-2011738. This work was supported by the National Science Foundation (NSF), under NSF DMR (Award No. 1461499) with support from NSF CREST 1547830 and 2112550. C. K. McGinn gratefully acknowledges funding via the National Science Foundation Graduate Research Fellowship Program.

AUTHOR DECLARATIONS

Conflict of Interest

The authors have no conflicts to disclose.

Author Contributions

Christine K. McGinn: Conceptualization (equal); Data curation (equal); Formal analysis (lead); Investigation (lead); Methodology (lead); Writing – original draft (lead). **Nasim Fahramand:** Data curation (supporting); Formal analysis (supporting); Investigation (supporting); Methodology (supporting); Writing – review & editing (equal). **Stephen O'Brien:** Conceptualization (equal); Data curation (supporting); Formal analysis (supporting); Investigation (supporting); Methodology (supporting); Supervision (equal); Writing – review & editing (equal). **Ioannis Kymissis:** Conceptualization (equal); Formal analysis (supporting); Project administration (lead); Supervision (equal); Writing – review & editing (equal).

DATA AVAILABILITY

The data that support the findings of this study are available from the corresponding author upon reasonable request.

REFERENCES

[1]A. A. Nayl, A. I. Abd-Elhamid, A. Y. El-Moghazy, M. Hussin, M. A. Abu-Saied, A. A. El-Shanshory, and H. M. Soliman, "The nanomaterials and recent progress in biosensing systems: A review," Trends Environ. Anal. Chem. **26**, e00087 (2020).
[2]M. Li, T. Chen, J. J. Gooding, and J. Liu, "Review of carbon and graphene quantum dots for sensing," ACS Sens. **4**, 1732–1748 (2019).
[3]R. W. Epps, M. S. Bowen, A. A. Volk, K. Abdel-Latif, S. Han, K. G. Reyes, A. Amassian, and M. Abolhasani, "Artificial chemist: An autonomous quantum dot synthesis bot," Adv. Mater. **32**, 1–9 (2020).
[4]R. A. Surmenev, T. Orlova, R. V. Chernozem, A. A. Ivanova, A. Bartasyte, S. Mathur, and M. A. Surmeneva, "Hybrid lead-free polymer-based nanocomposites with improved piezoelectric response for biomedical energy-harvesting applications: A review," Nano Energy **62**, 475–506 (2019).
[5]J. C. Y. Kenry and C. T. Lim, "Emerging flexible and wearable physical sensing platforms for healthcare and biomedical applications," Microsyst. Nanoeng. **2**, 16043 (2016).
[6]A. Toprak and O. Tigli, "Comprehensive characterization of PVDF-TrFE thin films for microelectromechanical system applications," J. Mater. Sci.: Mater. Electron. **28**, 15877–15885 (2017).
[7]C. Ribeiro, C. M. Costa, D. M. Correia, J. Nunes-Pereira, J. Oliveira, P. Martins, R. Gonçalves, V. F. Cardoso, and S. Lanceros-Méndez, "Electroactive poly(vinylidene fluoride)-based structures for advanced applications," Nat. Protoc. **13**, 681–704 (2018).
[8]L. Li, J. Zheng, J. Chen, Z. Luo, Y. Su, W. Tang, X. Gao, Y. Li, C. Cao, Q. Liu, X. Kang, L. Wang, and H. Li, "Flexible pressure sensors for biomedical applications: From ex vivo to in vivo," Adv. Mater. Interfaces **7**, 2000743 (2020).
[9]B. Stadlober, M. Zirkl, and M. Irimia-Vladu, "Route towards sustainable smart sensors: Ferroelectric polyvinylidene fluoride-based materials and their integration in flexible electronics," Chem. Soc. Rev. **48**, 1787–1825 (2019).
[10]Y. Yu, H. Sun, H. Orbay, F. Chen, C. G. England, W. Cai, and X. Wang, "Biocompatibility and in vivo operation of implantable mesoporous PVDF-based nanogenerators," Nano Energy **27**, 275–281 (2016).
[11]T. Q. Trung and N. E. Lee, "Flexible and stretchable physical sensor integrated platforms for wearable human-activity monitoringand personal healthcare," Adv. Mater. **28**, 4338–4372 (2016).
[12]Q. Shi, T. Wang, and C. Lee, "MEMS based broadband piezoelectric ultrasonic energy harvester (PUEH) for enabling self-powered implantable biomedical devices," Sci. Rep. **6**, 1–11 (2016).
[13]H. Gold, A. Petritz, E. Karner-Petritz, A. Tschepp, J. Groten, C. Prietl, G. Scheipl, M. Zirkl, and B. Stadlober, "Flexible single-substrate integrated active-matrix pyroelectric sensor," Phys. Status Solidi—Rap. Res. Lett. **13**, 1–8 (2019).
[14]M. Zirkl, B. Stadlober, and G. Leising, "Synthesis of ferroelectric poly(vinylidene fluoride) copolymer films and their application in integrated full organic pyroelectric sensors," in *Ferroelectrics* (Taylor and Francis Ltd., 2007), Vol. 353, pp. 173–185.
[15]Z. A. Lamport, M. R. Cavallari, K. A. Kam, C. K. McGinn, C. Yu, and I. Kymissis, "Organic thin film transistors in mechanical sensors," Adv. Funct. Mater. **2004700**, 1–19 (2020).
[16]X. Chen, X. Han, and Q. D. Shen, "PVDF-based ferroelectric polymers in modern flexible electronics," Adv. Electron. Mater. **3**, 1600460 (2017).
[17]R. Gregorio, M. Cestari, and F. E. Bernardino, "Dielectric behaviour of thin films of beta-PVDF/PZT and beta-PVDF/$BaTiO_3$ composites," J. Mater. Sci. **31**, 2925–2930 (1996).
[18]B. Ploss, B. Ploss, F. G. Shin, H. L. Chan, and C. L. Choy, "Pyroelectric or piezoelectric compensated ferroelectric composites," Appl. Phys. Lett. **76**, 2776–2778 (2000).
[19]H. I. Hsiang, K. Y. Lin, F. S. Yen, and C. Y. Hwang, "Effects of particle size of $BaTiO_3$ powder on the dielectric properties of $BaTiO_3$/polyvinylidene fluoride composites," J. Mater. Sci. **36**, 3809–3815 (2001).
[20]Z. M. Dang, H. Y. Wang, Y. H. Zhang, and J. Q. Qi, "Morphology and dielectric property of homogenous $BaTiO_3$/PVDF nanocomposites prepared via the natural adsorption action of nanosized $BaTiO_3$," Macromol. Rapid Commun. **26**, 1185–1189 (2005).
[21]S. D. Mahapatra, P. C. Mohapatra, A. I. Aria, G. Christie, Y. K. Mishra, S. Hofmann, and V. K. Thakur, "Piezoelectric materials for energy harvesting and sensing applications: Roadmap for future smart materials," Adv. Sci. **8**, 2100864 (2021).
[22]T. R. Shrout and S. J. Zhang, "Lead-free piezoelectric ceramics: Alternatives for PZT?," J. Electroceram. **19**, 111–124 (2007).

[23]S. Siddiqui, D. I. Kim, L. T. Duy, M. T. Nguyen, S. Muhammad, W. S. Yoon, and N. E. Lee, "High-performance flexible lead-free nanocomposite piezoelectric nanogenerator for biomechanical energy harvesting and storage," Nano Energy **15**, 177–185 (2015).
[24]J. S. Dodds, F. N. Meyers, and K. J. Loh, "Piezoelectric characterization of PVDF-TrFE thin films enhanced with ZnO nanoparticles," IEEE Sens. J. **12**, 1889–1890 (2012).
[25]T. Men, X. Liu, B. Jiang, X. Long, and H. Guo, "Ferroelectric β-crystalline phase formation and property enhancement in polydopamine modified $BaTiO_3$/poly (vinylidene fluoride-trifluoroethylene) nanocomposite films," Thin Solid Films **669**, 579–587 (2019).
[26]S. Gupta, D. Shakthivel, L. Lorenzelli, and R. Dahiya, "Temperature compensated tactile sensing using MOSFET with P(VDF-TrFE)/$BaTiO_3$ capacitor as extended gate," IEEE Sens. J. **19**, 435–442 (2019).
[27]L. Gloag, M. Mehdipour, D. Chen, R. D. Tilley, and J. J. Gooding, "Advances in the application of magnetic nanoparticles for sensing," Adv. Mater. **31**, 1–26 (2019).
[28]S. Gupta, L. Lorenzelli, and R. Dahiya, "Multifunctional flexible PVDF-TrFE/$BaTiO_3$ based tactile sensor for touch and temperature monitoring," in *Proceedings of IEEE Sensors* (IEEE, 2017), Vol. 2017, pp. 1–3.
[29]M. Xie, K. Hisano, M. Zhu, T. Toyoshi, M. Pan, S. Okada, O. Tsutsumi, S. Kawamura, and C. Bowen, "Flexible multifunctional sensors for wearable and robotic applications," Adv. Mater. Technol. **4**, 1–29 (2019).
[30]I. Graz, M. Krause, S. Bauer-Gogonea, S. Bauer, S. P. Lacour, B. Ploss, M. Zirkl, B. Stadlober, and S. Wagner, "Flexible active-matrix cells with selectively poled bifunctional polymer-ceramic nanocomposite for pressure and temperature sensing skin," J. Appl. Phys. **106**, 034503 (2009).
[31]H. S. Nalwa, "A review of molybdenum disulfide (MoS_2) based photodetectors: From ultra-broadband, self-powered to flexible devices," RSC Adv. **10**, 30529–30602 (2020).
[32]C. J. Murphy, "Optical sensing with quantum dots," Anal. Chem. **79**, 521–526 (2002).
[33]K. Wu, D. Su, R. Saha, J. Liu, V. K. Chugh, and J.-P. Wang, "Magnetic particle spectroscopy: A short review of applications using magnetic nanoparticles," ACS Appl. Nano Mater. **3**, 4972–4989 (2020).
[34]L. Gloag, M. Mehdipour, D. Chen, R. D. Tilley, and J. J. Gooding, "Advances in the application of magnetic nanoparticles for sensing," Adv. Mater. **31**, 1904385 (2019).
[35]N. Farahmand, C. K. McGinn, Q. Zhang, Z. Gai, I. Kymissis, and S. O'Brien, "Magnetic and dielectric property control in the multivalent nanoscale perovskite $Eu_{0.5}Ba_{0.5}TiO_3$," Nanoscale **13**, 10365–10384 (2021).
[36]C. K. McGinn, N. Farahmand, I. Kymissis, and S. O'Brien, "Morphology of small diameter barium titanate nanoparticle and polyvinylidene diflouride-trifluoroethylene composites," in *2021 IEEE International Symposium on Applications of Ferroelectrics (ISAF)* (IEEE, 2021), pp. 1–4.
[37]D. Setiadi, T. D. Binnie, P. Regtien, and M. Wubbenhorst, "Poling of VDF/TrFe copolymers using a step-wise method," in *9th International Symposium on Electrets, 1996* (ISE 9) (IEEE, 1996), pp. 831–835.
[38]P. Martins, A. C. Lopes, and S. Lanceros-Mendez, "Electroactive phases of poly(vinylidene fluoride): Determination, processing and applications," Prog. Polym. Sci. **39**, 683–706 (2014).
[39]R. Herdier, D. Jenkins, E. Dogheche, D. Rèmiens, and M. Sulc, "Laser Doppler vibrometry for evaluating the piezoelectric coefficient d_{33} on thin film," Rev. Sci. Instrum. **77**, 093905 (2006).